ResearchGate

See discussions, stats, and author profiles for this publication at:
https://www.researchgate.net/publication/257526870

Image based kinetic determination of iron (III) in blood samples using a CCD camera

ARTICLE *in* REACTION KINETICS, MECHANISMS AND CATALYSIS · OCTOBER 2012

Impact Factor: 1.17 · DOI: 10.1007/s11144-012-0453-1

CITATION
1

READS
25

4 AUTHORS, INCLUDING:

Maryam Khoshkam
Institute for Advanced Studi…

9 PUBLICATIONS **39** CITATIONS

SEE PROFILE

Available from: Maryam Khoshkam
Retrieved on: 02 February 2016

Reac Kinet Mech Cat (2012) 107:49–61
DOI 10.1007/s11144-012-0453-1

Image based kinetic determination of iron(III) in blood samples using a CCD camera

M. Kompany-Zareh · H. Tavallali · N. Shakernasab · M. Khoshkam · E. Shamsdin

Received: 27 November 2011 / Accepted: 1 May 2012 / Published online: 30 May 2012
© Akadémiai Kiadó, Budapest, Hungary 2012

Abstract Digital image-based calibration was applied for the determination of iron(III), Fe^{3+}, as a catalyst in the oxidation of indigo carmine (IC) using bromate ion (BrO_3^-). During the reaction, a colorless product was produced and there was an induction period (IP) before the color of the solution faded. The length of IP depended on the concentration of Fe^{3+}. The color fading of reaction was recorded as a change of red, blue and green colors (%RBG). Kinetic profiles similar to what has been reported in a previous spectrophotometric study were obtained. Fe^{3+} was determined in the concentration range of 6–16 ppm at pH = 2 and 25 °C. The detection limit of Fe^{3+} was found to be 1.994 ppm, which is better in comparison with the previous work. Optimum concentrations of IC and BrO_3^- were obtained as 5.5×10^{-5} and 3×10^{-3} M, respectively, using a one-at-a-time optimization method. The optimum pH value was 2. The interference effect of various cations and anions on the determination of iron is reported. In addition, the application of the method to real samples of human serum was performed. The obtained results from real samples were in accordance with the obtained results using standard methods. The analysis of images (movies) recorded from an evolutionary chemical systems seems to open new, simple and low-cost analytical opportunities.

Keywords Kinetic · Image analysis · CCD camera · Iron(III) · Determination · Interference

M. Kompany-Zareh (✉) · M. Khoshkam
Departments of Chemistry, Institute for Advanced Studies in Basic Sciences (IASBS), GavaZang 45137-66731, Zanjan, Iran
e-mail: kompanym@iasbs.ac.ir

H. Tavallali · N. Shakernasab · E. Shamsdin
Department of Chemistry, Payame Noor University, 71365-944 Shiraz, Iran

Introduction

Quantitative determination using spectrophotometric techniques is one of the most important purposes in data analysis. Most spectrophotometric techniques are based on the measurement of the light transmitted by analyte. The main disadvantage of a commercial spectrophotometer is that it is expensive and bulky [1]. The use of digital imaging as a detector for colorimetric reactions has great potential for many applications which involve the production of chemical color changes [2]. In addition, these methods are fast, simple and cheap [3]. There are different types of cameras such as mobile phone camera [1], TV camera [1, 4, 5] and digital camera [3, 6, 7], which have been reported as a detector for analyzing chemical systems [1]. Using a camera as a detection system can replace the more expensive colorimetric or fluorometric based methods in spectrophotometers or fluorometers, respectively [1, 8, 9].

Digital cameras are based on complementary metal oxide semiconductor (CMOS) or charge-coupled device (CCD) sensor technologies, which can record digital images and represent a current opportunity to develop fast and direct quantitative determinations for analytical chemistry. The quality of obtained images from CCD cameras are better than those obtained from CMOS systems but the latter are smaller, faster and can be produced cheaper [1]. The color and intensity data as obtained by the camera are usually 24 bit data. These are three colors: red (R), green (G) and blue (B). The intensity of each color has eight bits or 256 levels. In this color scheme $256 \times 256 \times 256 = 16{,}777{,}216$ colors are obtained and the value zero refers to black and 16,777,215 is pure white. Other colors are in between, which have no resemblance to the white light spectrum [10].

However, CCD cameras have been more widely used as detectors because of their earlier and more mature development [1]. Imaging is not new to science and has been widely used. Since the 1970s, many imaging devices have been developed having different detector configurations—an example is the established CCD sensor [11]. Information derived from images is useful in solving a number of questions related to subjects like material sciences, medicine and industrial processes; food and pharmaceutical quality control. Thus, images can be used as a source of information especially when converted to matrices. They are used in many areas of science [10, 12]. Gaiao et al. [3] used a CCD camera (webcam) as a novel technique for titration, named digital image-based (DIB) titration. The monitored signal in the DIB titration was an RGB based value. They determined HCl and H_3PO_4 in aqueous solutions and total alkalinity in mineral and tap waters. Maleki et al. [2, 10] used a CCD camera as a detector for the simultaneous determination of Al(III) and iron(III) in alloys. Safavi et al. [10] used a CCD camera as a full range pH sensor array. They determined TY, VB, SC, CR and NB indicators simultaneously. They studied the presence of Mg^{2+}, Hg^{2+}, Mn^{2+}, Ca^{2+} and Cd^{2+} ions as interference for free indicator using a CCD camera as detector. Lavigne et al. [10, 13] analyzed a series of polymer beads by a CCD camera. They determined species such as Ca^{2+}, Ce^{3+}, and simple sugars at different pH values. Although iron is only a trace element in biologic systems, it is the fourth most abundant element in the earth's crust and occurs in a variety of rock and soil minerals in oxidation states of two and three. It

has been proven that at low levels, iron is an essential element in the diet while at higher concentrations, it is toxic. A variety of sensitive analytical methods can be used for the determination of iron. Currently, some of the most common methods being used include spectrophotometry, chemiluminiscence, fluorescence analysis, polarographic and voltamperormetric analysis, flow injection analysis, atomic emission and atomic absorption spectrometry and others. Methods like catalytic kinetics are other well-designed alternatives, which could be used in the determination of trace elements. [14]. These methods have the advantage of combining high sensitivity using simple procedures and apparatus. Evidence in the form of reviews and experimental papers has shown that a number of kinetic methods have been used to determine iron at trace levels based on its catalytic action on the oxidation of various organic compounds. Oxidants such as hydrogen peroxide, or BrO_3^-, IO_4^-, and $S_2O_8^{2-}$ ions are frequently used and typical substrates are the aromatic amines, phenols and their derivatives [14].

This study is based on the reaction of IC and BrO_3^- involving the formation of an oxidized colorless product from blue IC indicator, for which iron(III) serves as a catalyst [15]. IC is a dye (C.I.NO. 73015) and is used as a redox indicator. Its oxidized form is produced by oxidants such as BrO_3^- in the presence of traces of iron. Iron(III) was determined based on its catalytic effect in IC oxidation by BrO_3^- anion. During the reaction, a colorless product was produced and there was an induction period (IP) before color fading of solution. The color fading of reaction was recorded as the change of red, blue and green colors (%RBG) received from a CCD camera as a color sensor instead of absorbance. Frames are taken by the CCD camera and are transferred to the computer. They were analyzed for red, green and blue components.

Experimental

Reagents and solutions

All of the utilized chemicals were of analytical grade chemicals. The buffer, reagent and stock solutions were prepared by doubly distillated water. A 1,000 ppm stock solution of Fe^{3+} was prepared by dissolving 0.3617 g of ($Fe(NO_3)_3 \cdot 9H_2O$, Merck) and diluted to 50 ml with distilled water. A stock solution of IC (1.0×10^{-3} M) was prepared by dissolving 0.0233 g of recrystalized IC (Merck) in 50 ml of distilled water. Buffer solutions of pH 1–5 were prepared by adding appropriate amounts of 0.1 M nitric acid (Merck) and 0.1 M acetic acid (pH 4) to sodium acetate 0.1 M (Merck), and the pH was measured with a pH meter. BrO_3^- solution (0.03 M) was prepared by dissolving 0.2505 g of $KBrO_3$ (Merck) in water in a 50 mL volumetric flask.

Instruments

A schematic diagram of the utilized system for recording the digital images is shown in Fig. 1a. A Canon sx110IS CCD (Charge Coupled Device) camera with

resolution equal to 96 dots per inch (dpi), 9 megapixel and (×10), which was positioned in front of a standard spectrophotometric glass cell with inner volume 4 ml and 1 cm optical path length, was used for recording of digital images. The colored solutions were only illuminated by light from a stable visible source. In order to minimize the effect of glare and specular reflection, the sample cells were put into a light-tight box with black internal walls and two holes in two sides, one of those for light entering and another for lens of camera location, as shown in Fig. 1a. The size of the box was $\sim 20 \times 15 \times 10$ cm The camera was connected to a Pentium III 650 MHz computer (PC). The pH values of buffer solutions were measured by a Jenway (3519) pH meter.

Recommended procedure

Calculation of RGB based data matrix

The considered catalytic reaction was followed in a cell during 5 min. In order to avoid interferences of stray lights and reflection from the walls and to provide a uniform illumination, the sample cell was put inside a dark box during the reaction time. First, the optimum conditions were obtained using a one-at-a-time optimization method. In this step, 6 ml of buffer with different pHs, different volumes from stock solutions of IC and BrO_3^- was diluted to 11.2 ml and then 0.1 ml from Fe^{3+} solution was added as a catalyst. Second, after finding the optimum conditions, in order to plot the calibration curve, 6 ml of the buffer

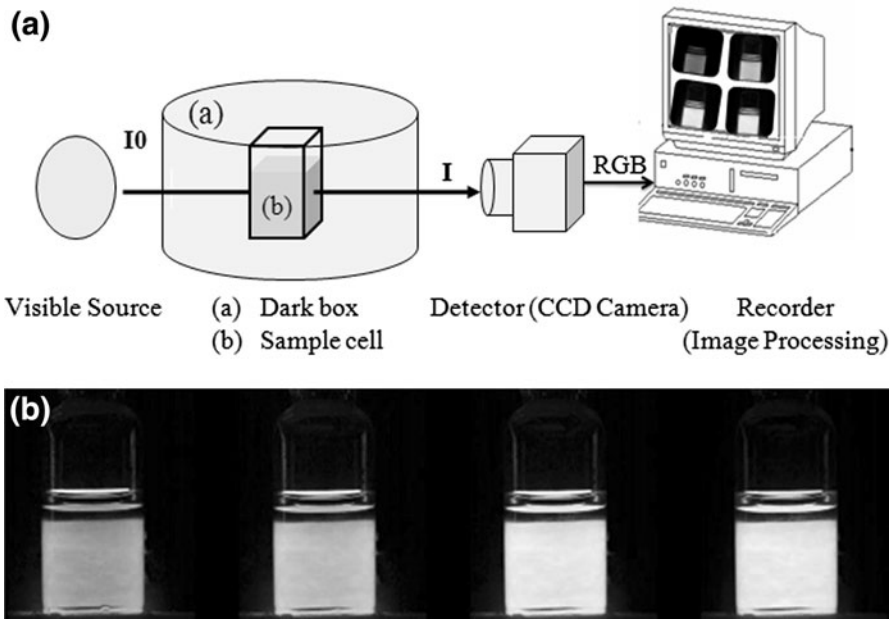

Figure 1 **a** Experimental setup, **b** image processing scheme

solution (pH = 2) was added to 0.80 ml from IC (1×10^{-3} M) and 1.0 ml from BrO_3^- (0.03 M) solutions, and the final solution was diluted to 11.2 ml by distilled water. After 10 s, different volumes from Fe^{3+} were added to the cell and the oxidation of colored solution to colorless solution was recorded immediately. Each experiment differed in the concentration of Fe^{3+} as a catalyst.

The applied procedure can be explained in three steps:

(1) The captured videos were transferred to computer using KMplayer software version 2.9.3.1428 and saved as an image in JPEG (middle) format and 0.24 frame/s speed. Then the frames were read via mfile which was written in MATLAB7. The size of each image was 120 × 80 and number of extracted frames was 90.

(2) A region, in which light beam crossed the reaction cell was selected with the computer mouse and this region was used for RGB based value calculation. Each sample image (frame) consist of 120 × 80 pixels and the selected region had a matrix with about 10 × 20 pixels. The pixel resolution was 96 dpi.

(3) A digitized color image was represented as an array of pixels, where each pixel contains numerical components that define a color. The images were converted to RGB values (the information of color was transformed into numbers). The size of each RGB image was (10 × 20 × 3) (where ten was the number of pixel rows, 20 was the number of pixel columns and three was the number of channels: *R*, *G* and *B*) Then the RGB values of each image were averaged. The final size of data set was (90 × 3) where 90 was the number of frames (time points) and in each time of reaction the data sets contained a 1 × 3 vector consisting of average of *R*, *G* and *B* values. In this technique, the three-dimensional RGB values of pixels of the images were taken as analytical signals.

Quantitative analysis

Quantitative results were obtained based on kinetic curves from R, G and B signals and using slope and induction period techniques [16].

The slope of variations in *R* values was very slow, whereas red color in the solution was rare. *B* values changed gradually, too, but their variation was obvious. In this method, the measured parameter was the amount of transmitted light from the solution to the camera as shown in Fig. 1a. The absorbance as a function of wavelength (Abs(λ)) can be calculated by the equation $\text{Abs}(\lambda) = -\log_{10}[I(\lambda)/I_0(\lambda)]$ where $I_0(\lambda)$ and $I(\lambda)$ are the spectral intensity of incident and transmitted rays, respectively, which can be obtained from the RGB values of digital color image for the reference sample. These kinetic curves based on absorbance were in accordance with the spectral response obtained in a previous paper using spectrophotometry [16]. Species involved in the reaction must have particularly good absorption properties in the visible wavelength region, thus, IC was a preferred candidate since the color of oxidized and reduced forms are different. The former has blue color and the latter is colorless.

Results and discussion

Analytical signals

The relationship between effective intensity and absorbance were calculated and are shown in Figs. 3, 4 and 5. Absorbance values were obtained using the equation $A = -\log(I/I_0)$, where I was the intensity of solution and I_0 was maximum intensity and equal to 256. Since the change in the red color was not desirable and irregular, we did not use it, and green and blue were used to draw the curves.

Effect of chemical variables

In this report, two different approaches, based on the slope (reaction rate) and induction period (*IP*), were employed on the measured data [16]. The rate of the color-fading during the oxidation of IC using BrO_3^- was characterized by the slope of the linear part in plot of the measured signal intensity versus time. The x axis in the plot is frame number that is representative of the reaction time. As the color faded, the signal (transmission) was increased and the linear part of the color-fading plot was prolonged (Fig. 2). The time corresponding to point P was defined as the induction period *IP* and was obtained from intersection of slope and the extrapolated line in the beginning of the process as shown in Fig. 2.

Many variables affect the rate of the reaction such as pH, IC and BrO_3^- concentrations. Thus, in the first part, these parameters were optimized one at a time and then the catalytic effect of Fe^{3+} was investigated.

The effect of IC concentration

The effect of IC concentration on the reaction rate and induction period of the reaction kinetic plot is shown in Fig. 3a. Increasing the concentration of IC as a redox

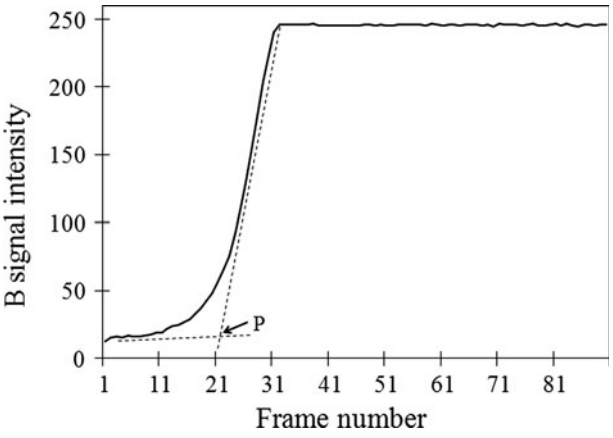

Figure 2 Change in the intensities of the B signal during the oxidation of IC (5.5×10^{-5} M) by BrO_3^- (5.0×10^{-3} M) in 6 ml buffer (pH = 2) and in the presence of 8 ppm of Fe^{3+}. The IP parameter is assigned as an intersection point P

indicator over the range of 1.5×10^{-5}–5.5×10^{-5} M, the reaction rate increased, but the induction period was almost unchanged. Both the slope and signal (RGB) intensity were higher when the concentration of IC increased. However, the optimum concentration of IC was chosen as 5.5×10^{-5} M in order to avoid nonlinearity due to the high color intensity of IC. A plot of the effect of IC concentration of the reaction rate using estimated absorptions is shown in Fig. 3b. The figure shows that as the reaction proceeds, the color of the solution fades and absorption decreases, which is opposite to what was observed for the signal intensity in Fig. 3a.

The effect of BrO_3^- ion concentration

The effect of BrO_3^- concentration on the reaction rate and induction period was investigated in the range of 1.8×10^{-3}–5.0×10^{-3} M, of BrO^{3-}. Fig. 4 shows that there is no significant increase in the reaction rate. However the induction period shortened with an increase in BrO_3^- concentration. Thus, 3.0×10^{-3} M of BrO_3^- was adopted for this work.

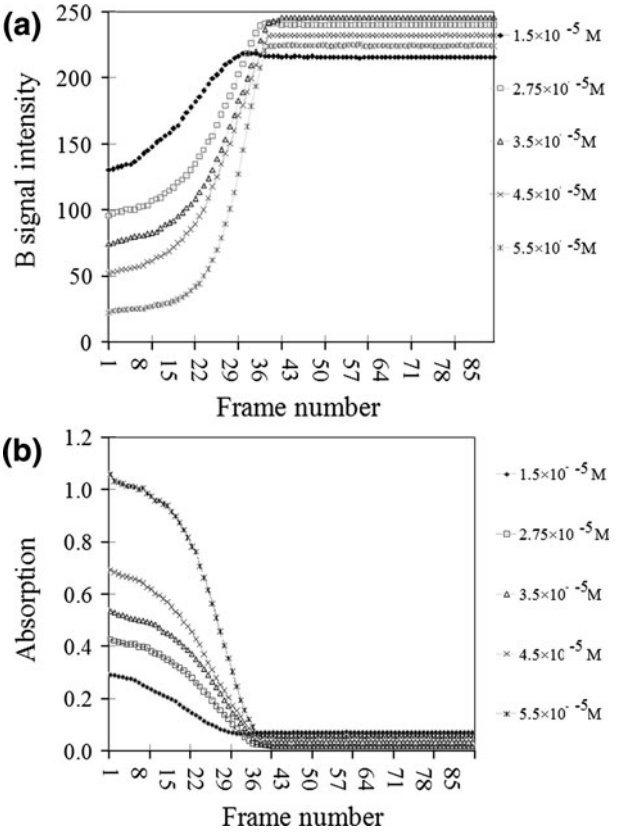

Figure 3 Effect of IC concentration on the reaction rate and IP in **a** intensities and **b** absorbances of the B signal in the presence of 6 ml buffer (pH = 2), 1 ml (0.03 M) BrO_3^- and 8 ppm Fe^{3+} as catalyst. Applied concentrations of IC were 1.5×10^{-5}, 2.75×10^{-5}, 3.5×10^{-5}, 4.5×10^{-5}, 5.5×10^{-5} M

The effect of pH on the reaction rate

In order to obtain the optimum conditions, the effect of pH on the reaction rate and induction period was investigated in the pH range 1.0–5.0, as shown in Fig. 5. As it can be seen, the high reaction rate and proper induction period were at pH = 2.0. So, pH 2.0 was used as optimum pH because higher sensitivity was achieved in the determination of Fe^{3+}.

In this way, the chosen optimum conditions were: pH equal to 2.0, IC concentration equal to 5×10^{-5} M and bromate concentration equal to 3×10^{-3} M.

Calibration graphs, precision, limits of detection and confidence limits

Calibration graphs were obtained by estimated absorption for average of R, G and B values of each curve in Fig. 6a and shown in Fig. 6b. They were linear in the range of 6–16 ppm of Fe^{3+}. Regression equations were equal to $y = -0.070x + 1.6218$

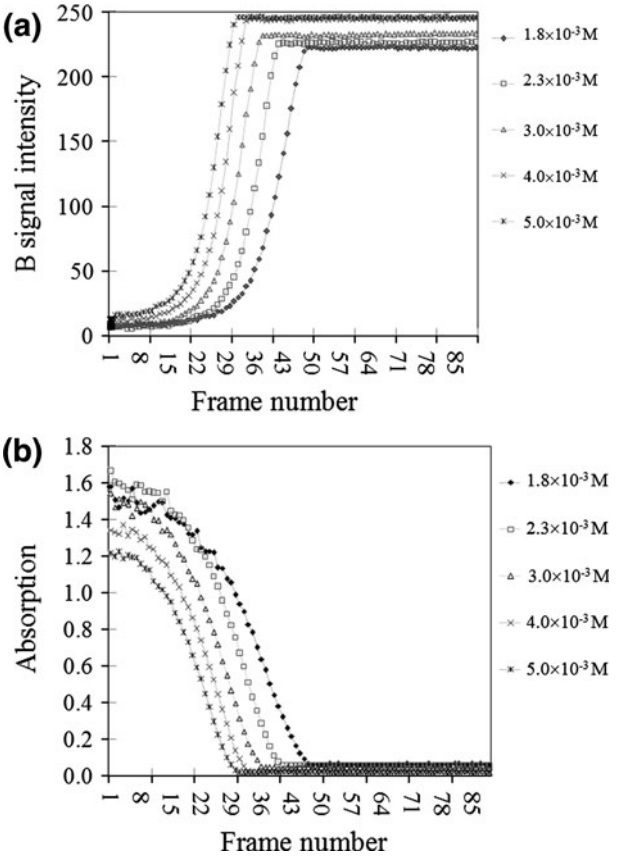

Figure 4 Effect of BrO_3^- concentration on the reaction rate and IP in **a** intensities and **b** absorbances of the B signal in the presence of 8 ppm of Fe^{3+}, 6 ml buffer (pH = 2) and 0.8 ml from IC (1.0×10^{-3} M) BrO_3^- concentrations were 1.8×10^{-3}, 2.3×10^{-3}, 3×10^{-3}, 4×10^{-3}, 5×10^{-3} M

with a correlation coefficient, $r^2 = 0.975$ for B signals; $y = -0.011x + 0.278$ and a correlation coefficient, $r^2 = 0.988$ for G signals; and $y = -0.010x + 0.185$ and a correlation coefficient, $r^2 = 0.994$ for R values, where x is the concentration of Fe^{3+} in ppm and y is the estimated absorbance.

The limit of detections for estimated absorbance in the B signal was 1.994 ppm**.** It can be calculated on the basis of $Y_{DL} = Y_B + 3S_B$ [17], in which Y_{DL}, Y_B, and S_B are signal of detection limit, blank signal, and standard deviation of the blank, inorder. The standard deviations of the slope (b) and intercept (a) in the regression line of B values were $S_b = 0.0056$ and $S_a = 0.0650$ [17]. The t value for ($n - 2 = 4$) degrees of freedom at 95% confidence level is 2.78. Thus the confidence limit at this level of certainty for slope (b) and intercept (a) were -0.0707 ± 0.0156 and 1.622 ± 0.180, respectively [17]. Table 1 shows the RSD values from ten replicates of each experiment in order to determine 6–16 ppm of Fe^{3+}, for B, G and R signals.

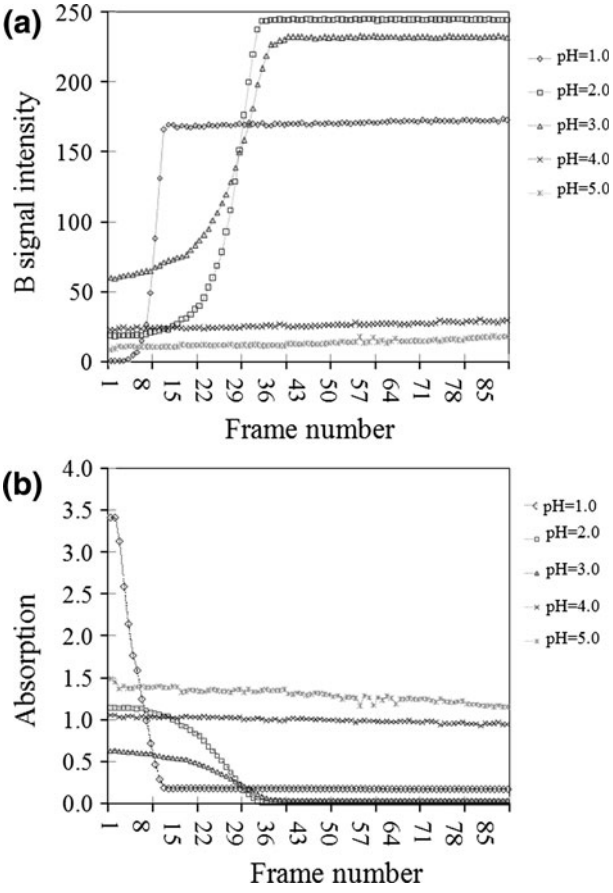

Figure 5 Effect of pH on the reaction rate and IP in **a** intensities and **b** absorbances of the B signal in the presence of 8 ppm of Fe^{3+}, 0.8 ml from IC (1.0×10^{-3} M), 1 ml BrO_3^- (0.03 M) and 6 ml buffer solution with different pHs (pH = 1–5)

Interference study

To study the selectivity of the proposed method, the effect of various cations and anions on the reaction rate and induction period of 5 ppm of Fe^{3+} was tested under the optimum conditions. The results are summarized in Table 2 with the maximum tolerance limit for each ion, in which the tolerance limits defined as the concentrations of iron causing a relative error of less than 2 %. Most of the cations and anions had no interfering effect. The tolerance limit of Ce^{4+} can be increased to 270 by the addition of 1 ml of 0.5 M KIO_3 in concentrated nitric acid to the sample solution and then filtering the ceric iodate. The interfering effect of F^-, I^- can be eliminated by addition of 1.0 ml of concentrated nitric acid to 10 ml of the sample solution and heating to dryness. With this procedure, the tolerance limit increased up to 200.

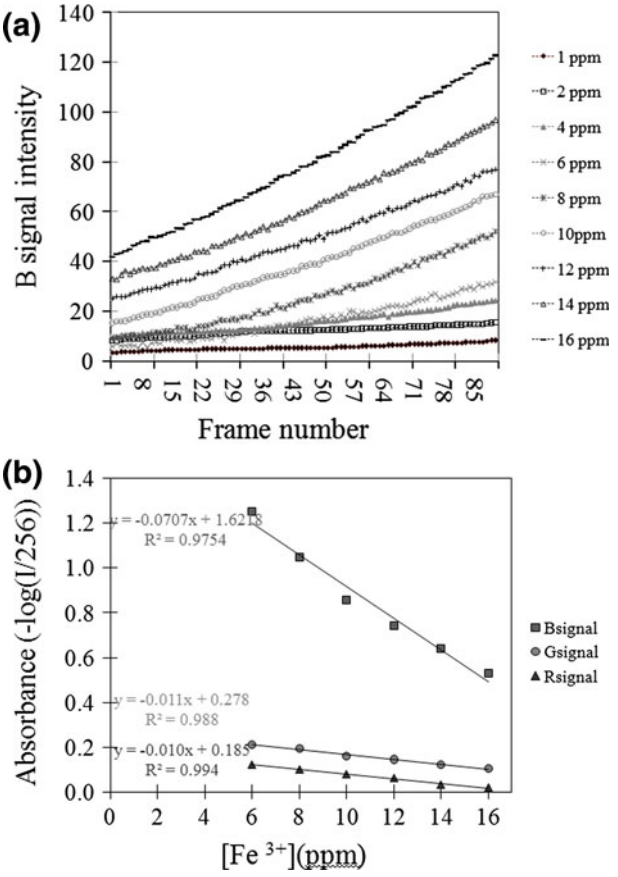

Figure 6 **a** Signal intensities (*B* values) versus frame numbers at different concentrations of Fe^{3+} under optimum conditions. The concentrations of BrO^{3-} and IC were 3×10^{-3} and 5.5×10^{-5} M, respectively, the pH of solutions was 2.0. The profiles of the kinetic curves were measured at various Fe^{3+} concentrations (1, 2, 4, 6, 8, 10, 12, 14 and 16 μg mL^{-1}). **b** Obtained calibration curve versus estimated absorption from signal intensity changes as a function of time (frame number). The considered signals were due to *B*, *G* and *R* values

Table 1 Relative standard deviation (RSD) of the *R*, *G* and *B* values in different concentrations of Fe^{3+}

Iron(III) concentration (ppm^{-1})	RSD (%) *B* values	RSD (%) *G* values	RSD (%) *R* values
1	0.35	0.25	5.44
2	0.44	0.16	2.65
4	0.32	0.41	2.21
6	0.39	0.80	4.36
8	0.28	0.86	3.42
10	0.36	0.71	3.31
12	0.25	0.62	3.13
14	0.32	0.59	3.09
16	0.23	0.69	2.64

RSD relative standard deviation for $n = 10$

Table 2 Effect of different ions as interference on the determination of 5 ppm Fe^{3+} under optimum conditions

Species	Tolerance limit of ion to iron (III) ($w_{ion}/w_{iron(III)}$)
Pb^{2+}, Ag^{+}, Ni^{2+}, Cd^{2+}, Se^{4+}	500[a]
Cu^{2+}, Mn^{2+}, Co^{2+}, IO_3^-	
Mg^{2+}	270
Cr^{3+}, Al^{3+}, ClO_4^-	200
Cl^-, CN^-, F^{-b}, I^{-b}	
NO_2^-, SCN^-	170
Sn^{2+}, V^{5+}, Mo^{6+}, Ce^{4+}	50
Hg^{2+}	20

[a] Largest amount tested

[b] After elimination of interference

Analysis of real sample

To evaluate the analytical applicability of the proposed method, the determination of Fe^{3+} in human serum was performed. For this purpose, 0.1 ml of blood serum was deproteinated by adding 0.1 ml of protein precipitant solution (CCl_3COOH). After 5 min, the mixture was centrifuged at 1,700 rpm for 15 min and 0.1 ml of the supernatant was diluted to 0.4 ml. Since the concentration range of iron in serum sample is lower than the DL of the method, proper volumes from the standard solution of iron were added to serum samples from 8 ppm for samples 1–4 and 10 ppm for samples 5 and 6, which were analyzed by the method proposed in this study as described above. The results after volume correction are summarized in Table 3, which gave satisfactory results that are comparable with atomic absorption spectrometry.

Conclusion

This work presents the first attempt to use image analysis for the kinetic determination of iron(III). The experiments showed that very good results can be achieved by simply using the RGB camera as a spectral based imaging device. It is noted that the methods described here would also be useful for the analysis of other

Table 3 Determination of iron(III) in human serum

Proposed method Iron(III) ppm	%(RSD)	AAS method Iron(III) ppm	%(RSD)
8.25	0.37	8.40	0.25
8.70	0.36	8.85	0.52
8.75	0.80	8.70	0.51
8.75	0.89	8.65	1.01
11.00	0.52	11.35	0.82
12.40	0.76	12.40	0.32

elements by adjusting the optimum conditions. The present method combines techniques already available, that is, instruments employed in this study, a video image analyzing system (CCD camera), and image analyzing computer software are those commonly used in typical chemical laboratories. This method gives a simple, low-cost, and sensitive determination of Fe^{3+} without the need for special equipment or time-consuming method. This is extremely attractive since the performance of existing CCD cameras can be enhanced without any requirements to modify the classical instrumentation. Adapting of conditions is very essential for gaining accurate results. Outcomes for image analysis were comparable to those acquired applying a usual spectrophotometer. This feasibility study showed very interesting results using a simple CCD camera in the laboratory for desirable observation. We are convinced it will provide new trends in analytical chemistry. Results suggest that we are able to determine Fe^{3+} spectrophotometry. We can say that image analysis is a proper way to determine the concentration iron(III). On the basis of these results, we believe that the development of low-cost spectral based imaging devices having performance very close to more expensive and complex multispectral devices will be possible in the future.

Acknowledgments The authors are grateful to Shiraz Payam Noor University for financial support of this study and Dr Charsoughi at Department of Physics in Institute for Advanced Studies in Basic Sciences (IASBS) for his kind collaboration in using of the software.

References

1. Wongwilai W, Lapanantnoppakhun S, Grudpan S, Grudpan K (2010) Webcam camera as a detector for a simple lab-on-chip time based approach. Talanta 81(3):1137–1141
2. Maleki N, Safavi A, Sedaghatpour F (2004) Single-step calibration, prediction and real samples data acquisition for artificial neural network using a CCD camera. Talanta 64(4):830–835
3. Gaiao EdN, Martins VL, Lyra WdS, Almeida LFd, Silva ECd, Araújo MCU (2006) Digital image-based titrations. Anal Chim Acta 570(2):283–290
4. Miyamoto T, Kuramitsu Y, Ookuma A, Trevanich S, Honjoh K, Hatano S (1998) Rapid detection and counting of viable bacteria in vegetables and environmental water using a photon-counting TV camera. J Food Protect 61:1312–1316
5. Akiyama M, Sugatani J, Suzuki Y, Miwa M (1994) Determination of platelet-activating factor acetylhydrolase activity by blotting, [beta]-radioluminescence, and ultrahigh-sensitivity television camera detection. Anal Biochem 218(2):295–299
6. Lopez-Molinero A, Liñan D, Sipiera D, Falcon R (2010) Chemometric interpretation of digital image colorimetry. Application for titanium determination in plastics. Microchem J 96(2):380–385

7. Ray E, Bunton P, Pojman JA (2007) Determination of the diffusion coefficient between corn syrup and distilled water using a digital camera. Am J Phys 75(10):903–906
8. Momeni N, Ramanathan K, Larsson PO, Danielsson B, Bengmark S, Khayyami M (1999) CCD-camera based capillary chemiluminescent detection of retinol binding protein. Anal Chim Acta 387(1):21–27
9. Cho I-H, Paek E-H, Kim Y-K, Kim J-H, Paek S-H (2009) Chemiluminometric enzyme-linked immunosorbent assays (ELISA)-on-a-chip biosensor based on cross-flow chromatography. Anal Chim Acta 632(2):247–255
10. Safavi A, Maleki N, Rostamzadeh A, Maesum S (2007) CCD camera full range pH sensor array. Talanta 71(1):498–501
11. Duponchel L, Milanfar P, Ruckebusch C, Huvenne J-P (2008) Super-resolution and Raman chemical imaging: from multiple low resolution images to a high resolution image. Anal Chim Acta 607(2):168–175
12. Borman S (1996) Array detectors are transforming optical spectroscopy ACS. Available via ACS. http://pubs.acs.org/cen/hotarticles/cenear/960318/array.html
13. Lavigne JJ, Savoy S, Clevenger MB, Ritchie JE, McDoniel B, Yoo S-J, Anslyn EV, McDevitt JT, Shear JB, Neikirk D (1998) Solution-based analysis of multiple analytes by a sensor array: toward the development of an "electronic tongue". J Am Chem Soc 120(25):6429–6430
14. Stoyanova A (2006) Spectrophotometric determination of iron(III) based on its catalytic effect on the oxidation of diphenylamine with hydrogen peroxide in the presence of cetylpyridinium chloride. J Univ Chem Technol Metall 41(2):205–210
15. Massoumi A, Tavallali H (1998) Kinetic spectrophotometric determination of vanadium by catalytic effect on the indigo carmine–bromate reaction. Anal Lett 31(1):193–206
16. Tavallali H, Massoumi A (1998) Simultaneous kinetic spectrophotometric determination of vanadium(V) and iron(III). Talanta 47(2):479–485
17. Miller JC, Miller JN (1993) Statistics for analytical chemistry. Ellis Horwood, New York